

Article

The Durability and Performance of Short Fibers for a Newly Developed Alkali-Activated Binder

Henrik Funke ^{1,*}, Sandra Gelbrich ² and Lothar Kroll ³

¹ Henrik Funke. Reichenhainer Str. 31/33, Chemnitz 09126, Germany

² Sandra Gelbrich. Reichenhainer Str. 31/33, Chemnitz 09126, Germany; sandra.gelbrich@mb.tu-chemnitz.de

³ Lothar Kroll. ul. Mikołajczyka 5, Opole 45-271, Poland; l.kroll@po.opole.pl

* Correspondence: henrik.funke@mb.tu-chemnitz.de; Tel.: +49-371-531-38995; Fax: +49-371-531-838995

Academic Editor: Edith Maeder

Received: 22 December 2015; Accepted: 9 March 2016; Published: 15 March 2016

Abstract: This study reports the development of a fiber-reinforced alkali-activated binder (FRAAB) with an emphasis on the performance and the durability of the fibers in the alkaline alkali-activated binder (AAB)-matrix. For the development of the matrix, the reactive components granulated slag and coal fly ash were used, which were alkali-activated with a mixture of sodium hydroxide (2–10 mol/L) and an aqueous sodium silicate solution ($\text{SiO}_2/\text{Na}_2\text{O}$ molar ratio: 2.1) at ambient temperature. For the reinforcement of the matrix integral fibers of alkali-resistant glass (AR-glass), E-glass, basalt, and carbon with a fiber volume content of 0.5% were used. By the integration of these short fibers, the three-point bending tensile strength of the AAB increased strikingly from 4.6 MPa (no fibers) up to 5.7 MPa (carbon) after one day. As a result of the investigations of the alkali resistance, the AR-glass and the carbon fibers showed the highest durability of all fibers in the FRAAB-matrix. In contrast to that, the weight loss of E-glass and basalt fibers was significant under the alkaline condition. According to these results, only the AR-glass and the carbon fibers reveal sufficient durability in the alkaline AAB-matrix.

Keywords: alkali-activated binder; fibers; durability; geopolymer

1. Introduction

The interest in the development of alternative building materials has been encouraged by the growth of the building industry and the increased performance requirements together with the higher sustainability criteria applied in civil engineering. Alkali-activated binders (AABs) represent an attractive alternative for the partial or complete substitution of Portland cement in the production of concrete and mortar. The potential benefits of the replacement of Portland cement by AABs are the reduction in carbon dioxide emissions. The production of 1 ton of Portland cement releases approximately 1 ton of carbon dioxide and requires about 100 kWh [1,2]. As opposed to this, the production of 1 ton of AABs generate only between 0.2 and 0.5 tons of carbon dioxide [3–5] and may be employed along with recycled aggregate for further reducing the environmental impact of concrete production (see, for instance, [6]). Beyond this, AABs point up a high mechanical strength, a high temperature and fire resistance, an acid resistance, and a low shrinkage [7–9].

Alkali-activated binders are prepared by the alkaline activation of aluminosilicate materials such as fly ash, granulated slag, and calcined clays [8,10], and cured at ambient or slightly higher temperature [11–13]. The alkaline activation, which comprises the solving process, polymerization and crystallization, depends on many parameters including chemical composition, physical properties (e.g., particle size distribution and specific surface area of the raw materials), composition of alkaline solution, and curing temperature [14,15].

For an enhancement of mechanical properties of the AAB, short fibers can be integrated [16,17]. The reinforcement of AABs by different fibers have not been widely reported. OHNO and LI studied the tensile and the compressive strength of randomly oriented short Poly-Vinyl-Alcohol (PVA) fiber-reinforced AABs [18]. PUERTAS *et al.* reported that incorporation of polypropylene fibers leads to an improvement of the compressive strength [19]. The influence of the fiber durability in an alkaline AAB-matrix has not been studied so far.

This paper presents results of the development of an AAB-matrix, and the measurement of the performance and durability of different fibers in the AAB-matrix. For that purpose, the durability of the fibers in an alkali solution is investigated. Additionally, the three-point bending tensile strength of the AABs in unreinforced and fiber-reinforced forms is studied.

2. Experimental Section

2.1. Components for Alkali Activated Binders

Table 1 presents the compositions of the alkali-activated binders. For the reactive binders, the coal fly ash (bulk density: 2.42 g/cm³) “EFA-Füller” (class F) by the company Bauminerale GmbH (Herten, Germany) and a granulated slag (bulk density: 2.85 g/cm³) by the company Holcim (Hamburg, Germany) were used. Table 2 shows the oxides compositions of the coal fly ashes and slag, which were determined by energy dispersive X-ray spectroscopy (EDX, Willich, Germany). The measured Blaine fineness of the coal fly ash and of the granulated slag was 7290 and 3740 cm²/g, respectively. A quartz sand (bulk density: 2.68 g/cm³) with a grain size of 0.1 to 1.0 mm was used as aggregate. The activator solutions consisted of a mixture of aqueous sodium silicate (SiO₂/Na₂O molar ratio: 2.1) and a solution of sodium hydroxide (bulk density: 1.55 g/cm³).

Table 1. Composition of AAB and OPCC in kg/m³.

Component	AAB	OPCC
Granulated slag	500	-
Coal fly ash	100	-
CEM I 52.5 R	-	500
Quartz sand 0–2 mm	1070	1780
NaOH-solution	340	-
Sodium silicate	100	-
plugging agent	4	-
Black pigment	10	-
superplasticizer	-	15
w/b	0.41	

Table 2. Oxides compositions of coal fly ash and granulated slag in wt%.

Oxide	Coal Fly Ash	Granulated Slag
SiO ₂	45	52
Al ₂ O ₃	10	30
Fe ₂ O ₃	-	10
CaO	35	5
MgO	10	3

The sodium hydroxide solution was prepared by dissolving sodium hydroxide pellets (99% purity, Merck KGaA, Darmstadt, Germany) in distilled water to a concentration of 2–10 mol/L and cooled to room temperature for 24 h. The water/binder ratio was 0.41. In this study, the alkali-activated binders were compared with an ordinary Portland cement concrete (OPCC).

2.2. Fibers for the Reinforcement of AAB-Matrix

Integral fibers of alkali-resistant glass (AR-glass), E-glass, basalt, and carbon with a fiber volume content of 0.5% were used for the reinforcement of the AAB-matrix (Table 3). The fibers were 12 mm long and had a fineness of 45 to 60 tex. All fibers had a sizing agent, whereby the content varied from 1.0% to 1.5% by mass (measured by thermogravimetry).

Table 3. Properties of the integral fibers.

Property	AR-glass	E-glass	Basalt	Carbon
Fineness in g/1000 m	45	52	60	50
Length in mm		12		
Content of sizing agent in wt%	1.1	0.9	1.5	1.2

2.3. Specimen Preparation

The sodium hydroxide solution and the aqueous sodium silicate were mixed via stirring for 15 min. After that, the AAB specimens were manufactured by adding the activator solutions to the solid precursor (fly ash and granulated slag) and the aggregate. Then, all specimens were produced by mechanical mixing for 4 min. Subsequently, the fibers were added to the fresh AAB and mixed together for 0.5 min. For the structural study of hardened AAB, the specimens were cast into corresponding molds and cured at a temperature of 20 °C and a relative humidity of 65% for 24 h. Subsequently, the samples used for the tests performed on the hardened concrete were stored dry, according to EN 12390-2.

2.4. Test Set-up

The compressive strength was determined by means of the Toni Technik ToniNorm (load frame 3000 kN) following EN 12390-3, with three cubes having an edge length of 150 mm (Figure 1a). The pre-load and the loading speed were 18 kN and 0.5 mm/min, respectively. The three-point bending tensile strength was determined by means of the Toni Technik ToniNorm (load frame 20 kN) with three samples measuring 160 × 40 × 40 mm³ (length × width × height), based on EN12390-5 (Figure 1b).

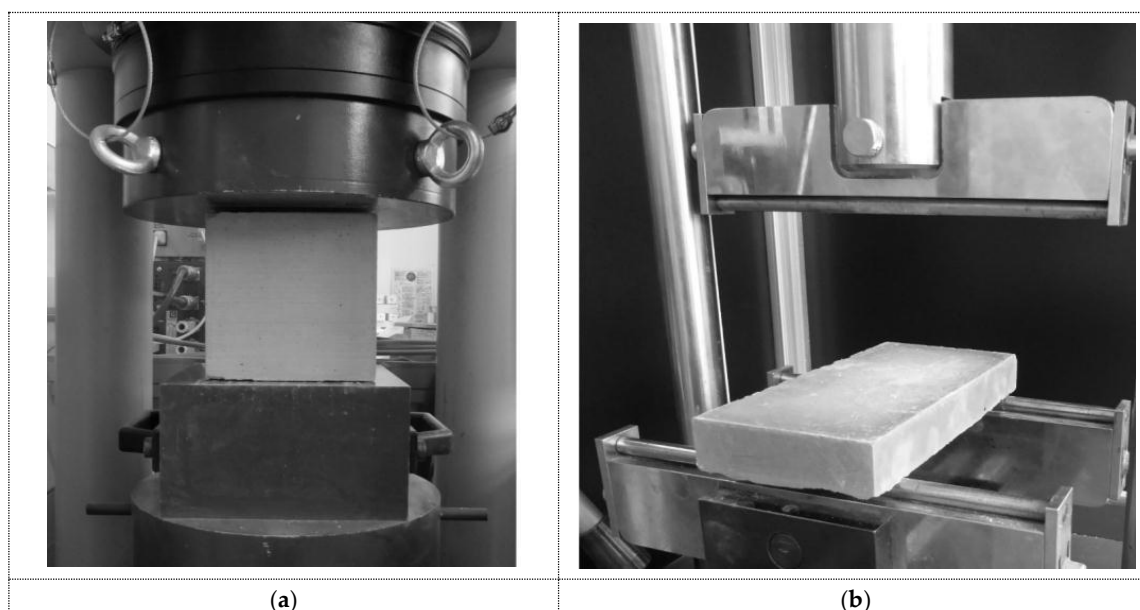


Figure 1. Determination of compressive strength (a) and three-point bending tensile strength (b).

In order to investigate the alkali resistance of the fibers in the AAB-matrix, the different types of fibers were immersed in a 1 mol/L solution of NaOH for 7, 14, 21, and 28 days at a temperature of 40

°C. After the periods of immersion, the eroded amount was quantitatively determined as a mass reduction based on weighing. For that purpose, the fiber samples were washed with distilled water and then dried for one day at a temperature of 60 °C before the weight losses were determined.

3. Results and Discussion

3.1. Basic Properties of Fresh and Hardened AAB

Table 4 shows the fresh and hardened AAB characteristics after 14 days. Using an air content tester, air content of 2.4 volume percent and a gross geometric density of 2.39 g/cm³ were determined in the fresh AAB. The compressive and the three-point bending tensile strength of the hardened AAB were 53.4 and 5.5 MPa, respectively. The total shrinkage deformation was 0.45 mm/m. The pH value of the fresh AAB was 14, whereby the pH value decreased to 10 due to the reactions in the hardened AAB. A dynamic elastic modulus of 36 GPa was determined by the ultrasonic examination.

Table 4. Basic properties of fresh and hardened AABs (NaOH: 5.5 mol/L).

Property	Fresh AAB	Hardened AAB
pH value	14	10
Geometric bulk density	2.39 g/cm ³	2.35 g/cm ³
Total shrinkage	0.45 mm/m	
Compressive strength	-	53.4 MPa
three-point bending tensile strength	-	5.5 MPa
Elastic modulus (dynamic)	-	36 GPa

In addition to the reactivity and the solids content of the alkali-activated binders, the amount and concentration of the alkaline activator have an influence on the solubility and reactivity of the AAB [20]. To demonstrate this influence, the three-point bending tensile strength (after seven days) is shown as a function of the NaOH concentration (1.2 to 10.0 mol/L) in Figure 2. Referring to Figure 2, an increase of the NaOH concentration leads to an increase of the three-point bending tensile strength. The sodium hydroxide concentration of over 5.5 mol/L did not further increase the three-point bending tensile strength, because the saturation point with respect to the solubility of the binder was reached, thus leading to a high level of degree of reaction.

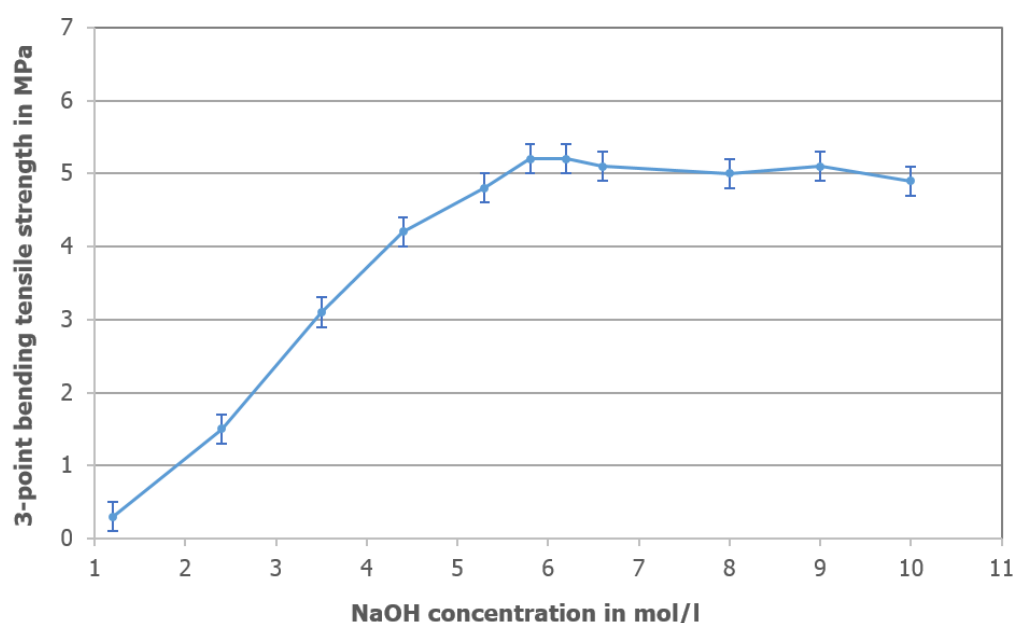


Figure 2. Three-point bending tensile strength as a function of the NaOH concentration.

3.2. Thermogravimetry

Figure 3 indicates the thermogravimetry and the differential thermogravimetry of the AAB-matrix. Regarding Figure 3, it can be observed that the weight loss started at a temperature of 35 °C with maximum weight loss at 87 °C. This weight loss can be attributed to the removal of free and unbound absorbed water molecules. The further mass loss up to a temperature of about 300 °C corresponded to the physically bound water in the porous matrix and the zeolite-water from the nanocrystalline zeolite structures [15,21,22]. The mass loss up to a temperature of around 520 °C resulted from the decomposition of the chemically bound water from the calcium silicate and the calcium aluminate phases. The cumulated weight loss was of 10.5% at a temperature of 900 °C.

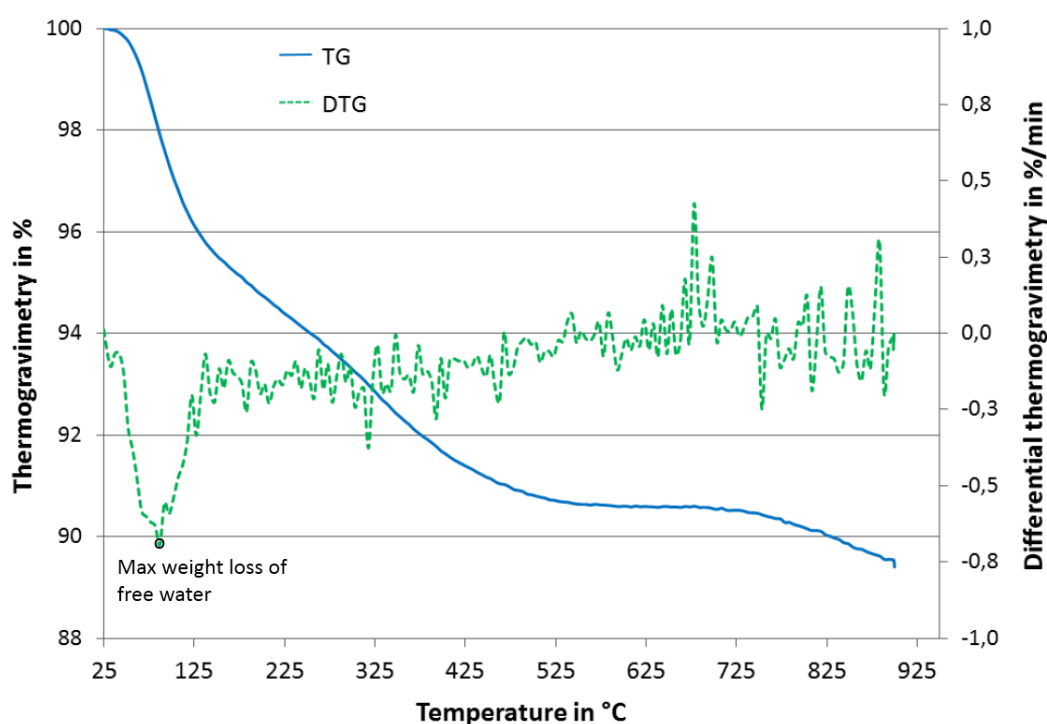


Figure 3. Thermogravimetry of alkali-activated binder matrix.

3.3. Durability and Performance of Fibers in the AAB-Matrix

Figure 4 shows the weight losses of the short fibers through the alkali attack after 7, 14, 21, and 28 days of the immersion in 1 mol/L NaOH. It was observed that the weight loss of E-glass and the basalt was significant under the alkaline condition (Figure 4). This is due to the fact that after 28 days the weight loss of the E-glass and the basalt were 9.8% and 14.7%, respectively. The high weight losses were due to the reaction between the SiO₂ in the E-glass and basalt fibers, and the alkaline solution. As opposed to that, the AR-glass showed a high alkali resistance, which was verified with a weight loss of only 1.8% after 28 days. The high durability of the AR-glass was caused by the reaction of zirconium oxide to the difficult soluble zirconium oxide hydrates, which interferes with the diffusion of hydroxide ions. Of all tested fibers, the carbon fibers showed the highest alkali resistance, with a weight loss of 0.9%.

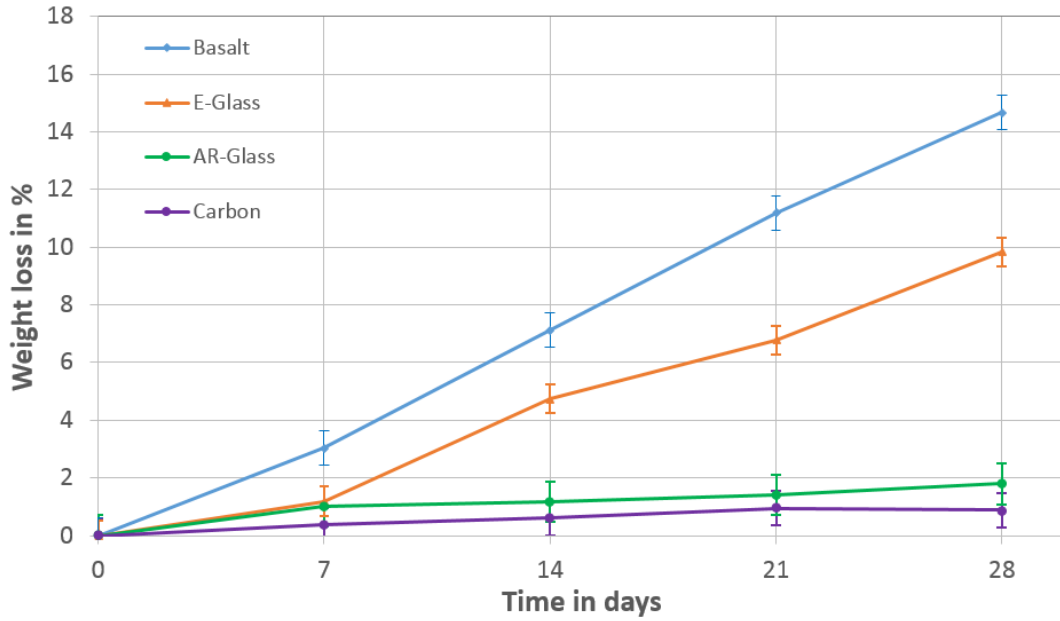


Figure 4. Weight losses of the fibers due to the alkaline attack.

Figure 5 indicates the three-point bending tensile strength of the fiber reinforced AAB-samples with respect to the exposition time of the samples. The AAB-sample without fibers had a three-point bending tensile strength of 4.6 MPa after one day (Figure 5), whereby the three-point bending tensile strength increased to 5.6 MPa after 28 days. By the integration of fibers, the three-point bending tensile strengths increased strikingly up to 5.7 MPa (carbon) after one day. After 28 days, the AR-glass and carbon fiber samples showed an increase of the three-point bending tensile strength of 6.8 and 7.3 MPa, respectively. Conversely, the strengths of the E-glass and the basalt fiber samples decreased after 7 days and 28 days to a three-point bending tensile strength of 5.8 and 5.6 MPa, respectively.

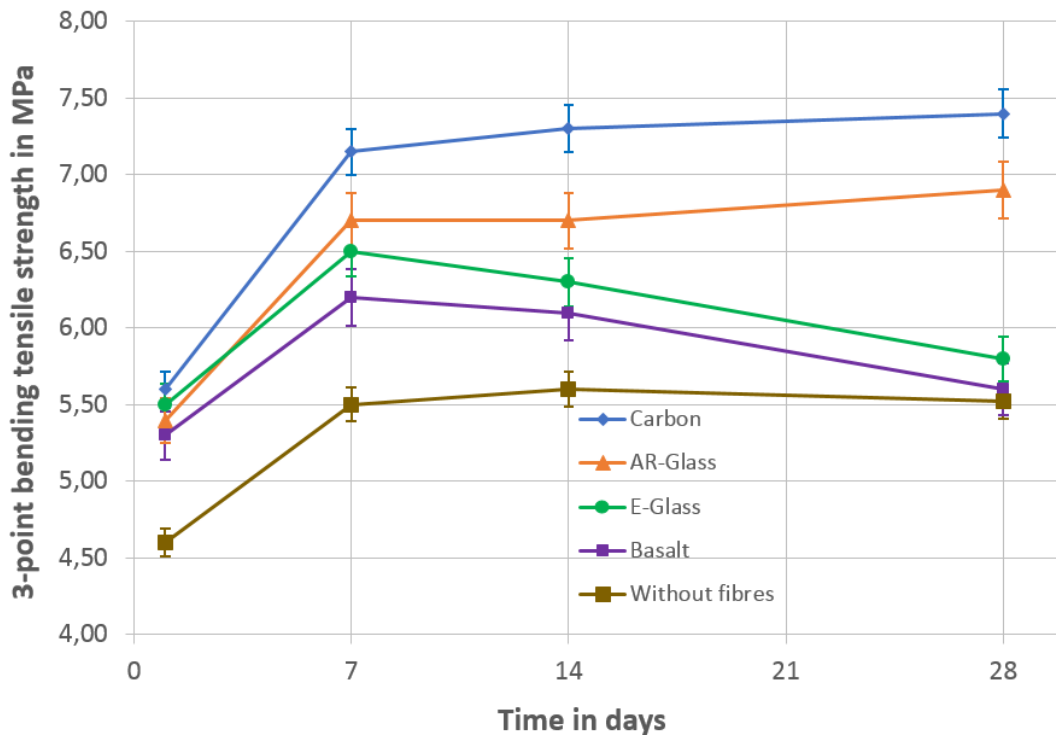


Figure 5. Performance of the fibers in the AAB-matrix as a function of time.

According to the results of the alkali resistance, the E-glass (Figure 6a) and the basalt fibers (Figure 6b) had similar fracture surfaces to the hardly visible pulled out fibers, and lost weight and strength more significantly than the AR-glass (Figure 6c) and the carbon fibers (Figure 6d) under the alkali immersion. The integration of E-glass and basalt fibers in the AAB-matrix resulted nearly in the same strength as the sample without fibers (Figure 6e) after 28 days (see Figure 5), which means these fibers degraded after 14 days due to the alkaline attack.

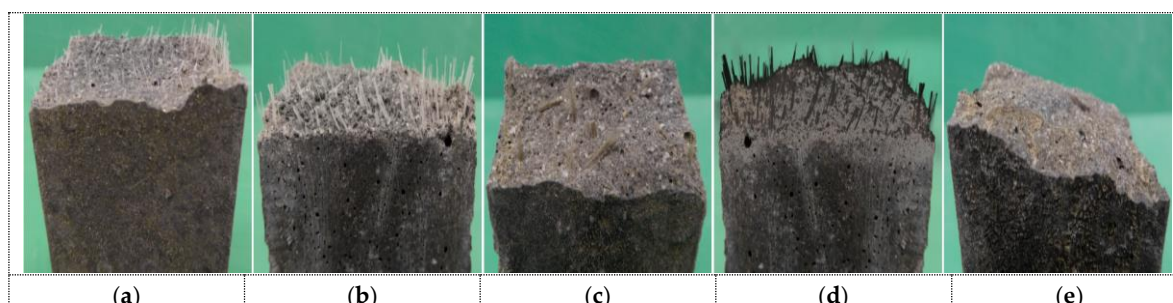


Figure 6. Test samples of the three-point bending tensile strength after 14 days. (a) E-glass; (b) AR-glass; (c) basalt; (d) carbon; (e) No fibers.

4. Conclusions

In this study, the development of an AAB-matrix and the performance and durability of different fibers in the AAB-matrix were investigated through various experimental works. Based on the results of this study, the following conclusions can be drawn:

- The adapted molarity for the saturation of the three-point bending tensile strength of the sodium hydroxide solution was 5.5 mol/L. Sodium hydroxide concentrations over 5.5 mol/L did not result in an increase of the three-point bending tensile strength after seven days.
- By the integration of short fibers, the three-point bending tensile strength of the AAB increased from 4.6 MPa (no fibers) up to 5.7 MPa (carbon) after one day.
- After 28 days, the three-point bending tensile strength of the AAB increased to 5.6 MPa (no fibers) and 7.3 MPa (carbon), which means an increase of 30%.
- The E-glass and the basalt fibers had similar deterioration under the alkali immersion and lost weight and strength more significantly than the AR-glass and the carbon fibers. According to this result, the E-Glass and the basalt fibers have no sufficient durability in the alkaline AAB-matrix.

This paper shows the potential of applying fiber-reinforced alkali-activated binder in civil engineering. The combination of alkali-activated binders and suitable fibers (e.g., carbon) results in an increase of the bending tensile strength of the AAB. Finally, the use of granulated slag and coal fly ash as binders for concrete and mortar reduce the environmental impact and may be employed along with recycled aggregate to further reduce the environmental impact of concrete production.

Acknowledgments: This work was supported by the Priority Program SPP 1542 of the German Research Foundation (DFG). The authors would like to acknowledge with gratitude the foundation's financial support.

Author Contributions: The manuscript was finalized through contributions from all authors and all authors approved the final manuscript.

Conflicts of Interest: The authors declare no conflict of interest.

References

1. Purnell, P. Material nature *versus* structural nurture: The embodied carbon of fundamental structural elements. *Environ. Sci. Technol.* **2011**, *46*, 454–61.
2. Cement Sustainability Initiative. Cement Technology Roadmap 2009. Carbon Emissions Reductions up to 2050; IEA: Paris, France, 2009.

3. McLellan, B.; Williams, R.; Lay, J.; van Riessen, A.; Corder, G. Costs and carbon emissions for geopolymer pastes in comparison to ordinary Portland cement. *J. Clean. Prod.* **2011**, *19*, 1080–1090.
4. Davidovits, J. Geopolymer cements to minimize carbon dioxide greenhouse warming. *Ceram. Trans.* **1993**, *37*, 165–826.
5. Komnitas, K.; Zaharaki, D. Geopolymerization: A review and prospects for the minerals industry. *Miner. Eng.* **2007**, *20*, 1261–1277.
6. Lima, C. Physical properties and mechanical behavior of concrete made with recycled aggregates and fly ash. *Cem. Concr. Res.* **2011**, *41*, 750–763.
7. Shi, C.; Jimenez, A.; Palomo, A. New cements for the 21st century: The pursuit of an alternative to Portland cement. *Constr. Build. Mater.* **2013**, *47*, 547–559.
8. Bernal, S.A. MgO content of slag controls phase evolution and structural changes induced by accelerated carbonation in alkali-activated binders. *Cem. Concr. Res.* **2014**, *57*, 33–43.
9. Funke, H.; Gelbrich, S. Alkalisch aktivierte Bindemittel zur Generierung von faserverstärkten Vergussmassen. In 19. Internationale Baustofftagung „Ibausil“, Weimar, Germany, 16–18 September 2015; pp. 859–866. (In German)
10. Damtoft, J. Sustainable development and climate change initiatives. *Cem. Concr. Res.* **2008**, *38*, 115–127.
11. Davidovits, J. Geopolymers: Inorganic polymeric new materials. *J. Therm. Anal.* **1991**, *37*, 1633–1656.
12. Cheng, T.W. Development and application of geopolymer technology: A review. *Min. Metall.* **2010**, *54*, 141–157.
13. Schneider, M. Sustainable cement production—Present and future. *Cem. Concr. Res.* **2011**, *41*, 642–650.
14. Duxson, P. The role of inorganic polymer technology in the development of green concrete. *Cem. Concr. Res.* **2007**, *37*, 1590–1597.
15. Duxson, P.; Lukey, G.; van Deventer, J. The thermal evolution of metakaolin geopolymers: Part 2—Phase stability and structural development. *J. Non Cryst. Solids* **2007**, *353*, 2186–2200.
16. Li, W.; Xu, J. Mechanical properties of basalt fiber-reinforced geopolymeric concrete under impact loading. *Mater. Sci. Eng.* **2009**, *505*, 178–186.
17. Funke, H.; Gelbrich, S.; Ehrlich, A.; Kroll, L. Rheological and mechanical development of a fiber-reinforced concrete for an application in civil engineering. *SOJ Mater. Sci. Eng.* **2014**, *2*, 1–4.
18. Ohno, M.; Li, V. A feasibility study of strain hardening fiber-reinforced fly ash based geopolymer composites. *Constr. Build. Mater.* **2014**, *57*, 163–168.
19. Puertas, F.; Amat, T.; Fernández-Jiménez, A.; Vázquez, T. Mechanical and durable behavior of alkaline cement mortars reinforced with polypropylene fibers. *Cem. Concr. Res.* **2003**, *33*, 2031–2036.
20. Buchwald, A. Der Einfluss des Kalziums auf die Kondensation von (Alumo-)Silikaten in alkali-aktivierten Binder. Habilitation Thesis, Fakultät Bauingenieurwesen, Bauhaus-Universität Weimar, Weimar, Germany, 2012. (In German)
21. Provis, J.; Lukey, G.; Deventer, J. Do Geopolymers Actually Contain Nanocrystalline Zeolites? A Reexamination of Existing Results. *Chem. Mater.* **2005**, *17*, 3075–3085.
22. Bernal, S. Mechanical and thermal characterization of geopolymers based on silicate activated metakaolin/slag blends. *J. Mater. Sci.* **2011**, *46*, 5477–5486.

